Behavioral/Cognitive

Neurophysiology of Effortful Listening: Decoupling Motivational Modulation from Task Demands

Frauke Kraus,[1,2] Bernhard Ross,[3,4] Björn Herrmann,[3,5]* and Jonas Obleser[1,2]*

[1]Department of Psychology, University of Lübeck, 23562 Lübeck, Germany, [2]Center of Brain, Behavior, and Metabolism, University of Lübeck, 23562 Lübeck, Germany, [3]Rotman Research Institute, Baycrest Academy for Research and Education, Toronto, Ontario M6A 2E1, Canada, [4]Department of Medical Biophysics, University of Toronto, Toronto, Ontario M5G 1L7, Canada, and [5]Department of Psychology, University of Toronto, Toronto, Ontario M5G 1L7, Canada

In demanding listening situations, a listener's motivational state may affect their cognitive investment. Here, we aim to delineate how domain-specific sensory processing, domain-general neural alpha power, and pupil size as a proxy for cognitive investment encode influences of motivational state under demanding listening. Participants (male and female) performed an auditory gap-detection task while the pupil size and the magnetoencephalogram were simultaneously recorded. Task demand and a listener's motivational state were orthogonally manipulated through changes in gap duration and monetary-reward prospect, respectively. Whereas task difficulty impaired performance, reward prospect enhanced it. The pupil size reliably indicated the modulatory impact of an individual's motivational state. At the neural level, the motivational state did not affect auditory sensory processing directly but impacted attentional postprocessing of an auditory event as reflected in the late evoked-response field and alpha-power change. Both pregap pupil dilation and higher parietal alpha power predicted better performance at the single-trial level. The current data support a framework wherein the motivational state acts as an attentional top–down neural means of postprocessing the auditory input in challenging listening situations.

Key words: **cognitive demand; event-related field; gap detection; motivation intensity theory; neural alpha power; pupil dilation; reward prospect**

Significance Statement

How does an individual's motivational state affect cognitive investment during effortful listening? In this simultaneous pupillometry and magnetoencephalography study, participants performed an auditory gap-detection task while their motivational state was manipulated through varying prospect of a monetary reward. The pupil size directly mirrored this motivational modulation of the listening demand. The individual's motivational state also enhanced top–down attentional postprocessing of the auditory event but did neither change auditory sensory processing nor pregap parietal alpha power. These data suggest that a listener's motivational state acts as a late attentional top–down effect on auditory neural processes in challenging listening situations.

Introduction

The motivational state of a person influences whether they are willing to invest cognitively in demanding listening contexts (Brehm and Self, 1989; Richter et al., 2016; Kraus et al., 2023a). That is, a person who sees no intrinsic (e.g., enjoyment) or extrinsic (e.g., financial) value in listening and is thus in a low motivational state may be more likely to disengage from listening than someone who is highly motivated; especially so under highly demanding conditions (Brehm and Self, 1989; Pichora-Fuller et al., 2016; Richter et al., 2016; Herrmann and Johnsrude, 2020). When listening conditions are less demanding, a person may still engage in listening despite being little motivated (Brehm and Self, 1989; Richter et al., 2016). Although this interacting influence of task demands and motivation (Fig. 1*C*) is established theoretically and empirically, for example, for cognitive control tasks (Parro et al., 2018; Yee and Braver, 2018), little research has been conducted to investigate the impact of task demands and motivation on listening under challenges and to characterize the underlying neurophysiological mechanisms.

Received March 28, 2024; revised Aug. 7, 2024; accepted Aug. 8, 2024.

Author contributions: F.K., B.H., and J.O. designed research; F.K. performed research; B.R. contributed unpublished reagents/analytic tools; F.K., B.H., and J.O. analyzed data; F.K., B.H., and J.O. wrote the paper.

We thank Gloria Lai and Tazeen Atif for their assistance with data collection. This work was supported by Deutsche Forschungsgemeinschaft (DFG; Grant Number HE 7857/1-1) awarded to B.H. B.H is supported by the Natural Sciences and Engineering Research Council of Canada (Discovery Grant, RGPIN-2021-02602) and the Canada Research Chair program (CRC-2019-00156).

*B.H. and J.O. have joint senior authorship.

The authors declare no competing financial interests.

Correspondence should be addressed to Björn Herrmann at bherrmann@research.baycrest.org or Jonas Obleser at jonas.obleser@uni-luebeck.de.

https://doi.org/10.1523/JNEUROSCI.0589-24.2024

The noradrenergic (NE) modulation emerging from the locus ceruleus (LC) in the brainstem is one driver of pupil dilation (Joshi et al., 2016; Joshi and Gold, 2020). The LC–NE system is sensitive to attention (Vazey et al., 2018) and has a role in optimizing task performance and task engagement (Aston-Jones and Cohen, 2005a). Accordingly, pupil dilation as a proxy of LC–NE activity has often been used as an indicator of cognitive investment: the pupil dilates as a task becomes more difficult (Kahneman and Beatty, 1966; Zekveld et al., 2010; Koelewijn et al., 2012; Winn et al., 2015; Wendt et al., 2016; Ohlenforst et al., 2018; Kadem et al., 2020). Moreover, pupil size dynamics during high listening demands are known to be modulated by an individual's motivational state (Bijleveld et al., 2009; Zhang et al., 2019; Alfandari et al.,2023), recently confirmed by us using highly controlled noise stimuli (Kraus et al., 2023a) that will also be used in the present study. The motivation-driven additional cognitive investment indexed by pupil dilation predicted better behavioral outcomes (Kraus et al., 2023a).

Neural oscillatory alpha power is sensitive to listening demands, likely reflecting top–down attentional modulation (Weisz et al., 2011; Obleser et al., 2012; Petersen et al., 2015; Wöstmann et al., 2015; Dimitrijevic et al., 2017; Paul et al., 2021; Herrmann et al., 2023; Kraus et al., 2023b). However, in studies using highly controlled stimulus designs, in which task difficulty was manipulated without changing stimulus acoustics, an increase in alpha power has only been observed sometimes, for example, when relevant sound information occurs shortly after the stimulus onset (Herrmann et al., 2023), but not when relevant sound information occurs late in a stimulus and when visual stimuli are presented concurrently (Kraus et al., 2023b). Manipulating motivation orthogonally to task demands may help identifying the neural correlates of cognitive investment during listening. That is, neural activity in brain regions that mediate top–down control of attention (e.g., cingulate cortex) is modulated by motivation (Small et al., 2005). Consistently, occipital alpha power in a visual search task has been sensitive to monetary rewards (Sawaki et al., 2015), raising the possibility that alpha power may be modulated by a person's motivational state during listening and, in turn, providing an opportunity to identify the neural mechanisms underlying challenging listening.

Apart from neural signals possibly indexing attention networks directly, neural activity elicited by auditory stimuli may provide additional insights into motivation influences on neural processing during listening. Auditory sensory responses ~100 ms after the stimulus onset are enhanced as the saliency of a sensory input increases (for a review, see Näätänen and Picton, 1987) and when individuals attend to, compared with ignore, auditory stimuli (Hillyard et al., 1973) but effects of motivation have not been observed (Goldstein et al., 2006; Krebs et al., 2013). Motivation rather seems to modulate neural signals ~300 ms after the stimulus onset (Goldstein et al., 2006; Baines et al., 2011; van den Berg et al., 2014).

The current study will use magnetoencephalography (MEG) to investigate the neurophysiological changes associated with listening demands under different motivational states (using a reward manipulation). We will use pupil size data as a benchmark for modulatory influences of motivation on cognitive investment during listening (Kraus et al., 2023a). Using MEG, we will investigate whether reward prospect impacts auditory sensory processing and how reward prospect influences attentional processing under varying task demands (alpha power). In detail, we expect increased attentional processing under high motivation when listening is hard, but no additional motivational boost when listening is easy (Fig. 1*C*). Additionally, we will investigate the relationship among changes in the pupil size, sensory responses, and neural alpha power and to behavioral listening outcome.

Materials and Methods

Participants. Thirty-seven adults aged between 18 and 34 years participated in the current study (mean, 23.43 years; SD, 4.05 years; 11 males and 26 females; all right-handed). None of the participants reported having a history of neural disorders or hearing problems. Participants gave written informed consent before participation and received an honorarium of $15 CAD per hour. Their motivation was manipulated through financial rewards. Participants could earn an additional $15 CAD depending on their behavioral performance. The study was conducted at the Rotman Research Institute at the Baycrest Academy for Research and Education. The study protocols are in accordance with the Declaration of Helsinki and were approved by the local ethics committee of the Rotman Research Institute at the Baycrest Academy for Research and Education.

Experimental environment. MEG data were recorded with a 275-channel axial gradiometer MEG device (CTF-MEG Neuro Innovations) in an electromagnetically shielded room. Participants were placed in a seating position with their head centered in the MEG helmet. A back-projection screen was placed ~70 cm in front of participants. An eye-tracking camera (EyeLink 1000 Plus, SR Research) was mounted to the screen. The experimental stimulation was controlled by a laptop (Windows 10) running Psychtoolbox (version 3.0.14) in MATLAB. Sounds were presented via an external sound card (RME Fireface UCX II) and delivered binaurally via MEG-compatible insert earphones (E-A-RTONE 3A, 3M). A button response box was used to record participants' behavioral responses. After the MEG experiment, the location of the three fiducials (left tragus, right tragus, nasion) and the shape of the head were digitized using a 3-D digitizer (Polhemus FASTRAK).

Experimental design. The experimental design was similar to the one used in Kraus et al. (2023a). An auditory gap-detection task was chosen because the timing and degree of listening demand can be more tightly controlled than for speech materials that have been used in previous studies (Kraus et al., 2023a). In fact, our previous work shows effects of motivation on behavior and pupil size, and a critical interaction in line with theoretical frameworks (Brehm and Self, 1989; Richter et al., 2016; Fig. 1*C*), which studies using speech materials have not been able to observe. The experimental control afforded by the auditory gap-detection task (Henry and Obleser, 2012; Henry et al., 2014, 2017; Herrmann et al., 2023; Kraus et al., 2023a, b) facilitates the analysis of the interaction of motivation, listening demand, and listening outcome (Kraus et al., 2023a).

Participants were presented with 5.2 s white-noise sounds that each contained one gap (Fig. 1) and pressed a button with the right index finger on the response box as soon as they detected the gap. The gap could occur at 1 of the 70 randomly selected time points between 2.2 and 4.2 s after the noise onset (linearly spaced). Auditory stimuli were presented at 45 dB above the participant's sensation level, which was determined for each ear prior to the experiment using an audiometer. There was no visual stimulation during the presentation of the white noise. Participants were asked to keep their gaze on the black screen and not close their eyes.

The 2 × 2 design included the factors of task difficulty (easy, hard) and reward prospect (reward-irrelevant, reward-relevant). Task difficulty was manipulated via the duration of the gap in the noise sound. In the hard condition, gap duration was individually titrated to ~65% gap-detection performance in training blocks prior to the main experimental blocks (4–6 training blocks of 2 min each). Gaps in the easy condition were twice as long (Kraus et al., 2023a, b).

Half of the trials were paired with the possibility of receiving an additional financial reward based on the participant's performance on these

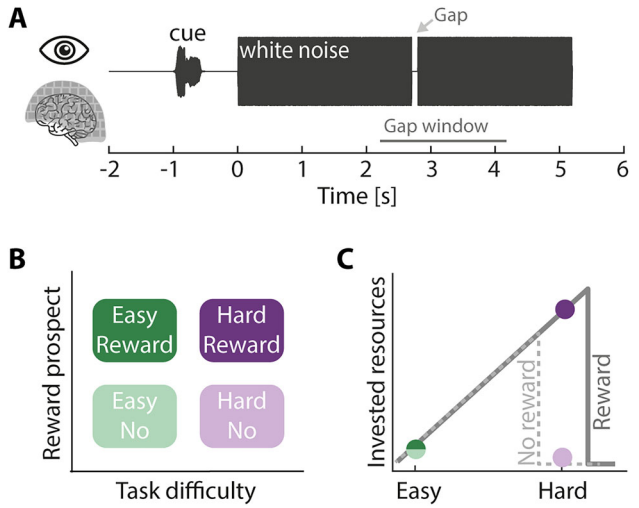

Figure 1. Experimental design. ***A***, Auditory gap-detection task: participants' task was to detect a gap within 5.2 s white-noise sound. The gap occurred randomly between 2.2 and 4.2 s postnoise onset (gap window, marked by the gray line). ***B***, Two-by-two design: task difficulty was determined by the gap duration (titrated to 65% detection performance for the hard condition and twice as long in easy trials). An auditory cue 1 s before each trial indicated whether the upcoming trial was reward-relevant or not. ***C***, Hypothesis: according to the Motivation Intensity Theory (gray lines; Brehm and Self, 1989; Richter, 2016), participants should invest cognitively under the hard listening condition only when motivated to succeed (solid line) but should give up investing resources when they are less motivated (dashed line). The colored dots show our hypothesis. Figure design follows Kraus et al. (2023a).

trials (reward-relevant trials). In contrast, the other half of the trials were not paired with any reward (reward-irrelevant trials). Specifically, after the experiment, three trials for each of the two difficulty levels were chosen from the reward-relevant trials (Tusche and Hutcherson, 2018; Teoh et al., 2020; Cole et al., 2022; Kraus et al., 2023a). Participants could gain $15 CAD in addition to their hourly compensation rate if their average performance across these six trials was above 80%. All of the participants reached this threshold and got the reward.

Trials were presented in 14 blocks, each containing 20 trials. In half of the blocks, task difficulty was easy, whereas task difficulty was hard in the other half. Easy and hard blocks alternated. The difficulty of the starting task was counterbalanced across participants. At the beginning of each block, participants received written information about the task difficulty (easy or hard) of the upcoming block. Hence, participants had prior knowledge about whether detecting the gap would be easy or hard. In a random order, half of the 20 trials per block were reward-relevant trials, whereas the other half were reward-irrelevant trials.

An auditory cue consisting of a guitar or a flute sound occurred before each white-noise sound, indicating whether a trial was reward-relevant or reward-irrelevant. The pairings of guitar and flute sound to reward-relevant and reward-irrelevant trials were counterbalanced across participants. Participants familiarized themselves with the cue–reward association during training trials before the experiment. Overall, the experiment contained 70 white-noise sounds per task difficulty (easy, hard) × reward prospect (reward-irrelevant, reward-relevant) condition, resulting in 280 trials.

After the experiment, participants completed a questionnaire regarding their use of the reward cues. They first indicated which auditory cue was associated with reward-relevant trials. We then asked them to rate the following statement: "I used the auditory cues (guitar and flute) to distinguish between important and unimportant conditions" on a six-point scale ranging from "strongly disagree" over "disagree," "somewhat disagree," "somewhat agree," and "agree" to "strongly agree." Participants rated this statement twice, separately for the easy and the hard conditions.

Analysis of behavioral data. Any button press within 0.1 to 1.5 s after the gap onset was defined as a hit (coded 1). Trials for which no button was pressed within this time window were considered a miss (coded 0). The time between the gap onset and the button press was calculated as the response time. The time at which the gap occurred within the sound was included in the statistical modeling (see below, Statistical analysis) to account and test for an expected hazard effect (higher accuracy and faster response times for later compared with early gaps relative to white-noise onset; Niemi and Näätänen, 1981; Nobre et al., 2007; Herrmann et al., 2023). Response-time data were log-transformed for statistical analysis to obtain values closer to a normal distribution.

Pupil data recording and preprocessing. Eye movements and pupil size of the right eye were continuously recorded using an EyeLink 1000 Plus eye tracker (SR Research). Data were recorded as an additional channel of the MEG data acquisition. MATLAB (MathWorks) was used for the preprocessing and analyses of the data. To detect eyeblinks, we determined the threshold in the pupil channel above which the eye tracker had lost the pupil in case of a blink. All data points above this threshold were coded as invalid (NaN). Additionally, 100 ms before and 200 ms after above threshold time points were also coded as NaN. NaN-coded data points were linearly interpolated. Pupil data were subsequently low-pass filtered at 4 Hz (Butterworth, fourth order) and divided into epochs ranging from −2 to 6.2 s time-locked to the white-noise onset. An epoch was excluded if >40% of the trial had been NaN-coded prior to interpolation. If >50% of the trials in any condition were excluded, the full pupil dataset of the respective participant was excluded from analysis ($N = 12$). The high number of excluded pupil datasets is in part due to the technical challenge combining the concurrent recording of the pupil size and MEG. Pupil size data were downsampled to 50 Hz. The polarity of the pupil data was inverted at the analysis stage because the pupil recordings through the MEG were inverted (we determined this in a brief black vs white screen experiment to elicit dilation vs constriction, respectively). For each trial, the mean pupil size in the −1.5 to −1.1 s time window was subtracted from the pupil size at every time point of the epoch (baseline correction). This baseline time window was chosen to avoid contamination of the auditory cue which was presented at −1 s. For each participant, single-trial time courses were averaged, separately for each condition.

Pupil size analysis. For the statistical analysis (described below, Statistical analysis) of the effects of task difficulty and reward prospect, pupil size data were averaged across the time window ranging from 2.2 s (onset of gap window) to 6.2 s (end of trial).

Similar to our previous approach (Kraus et al., 2023a), we investigated whether a smaller pupil size is associated with an increased probability that a participant misses a gap or responds slower to the gap. Therefore, pupil size data (baseline-corrected to −1.5 to −1.1 s to the noise onset) were time-locked to the gap onset. For statistical analysis, the pupil size was averaged across the −0.5 to 0 s time window, time-locked to the gap onset.

To illustrate the association between the pupil size and response time (Fig. 3*E*), we created two groups of trials: fast and slow trials. Fast trials were defined as those with response times equal to or faster than 0.75 SD of the mean. Slow trials were defined as those with response times equal to or slower than 0.75 SD of the mean. The threshold was chosen as a good compromise between too many and too few trials per group. The grouping was done separately for reward-relevant and reward-irrelevant trials to ensure the same number of trials was used for each group and reward condition. Additionally, we included only trials into the group of fast trials if their gap-onset time matched with one trial of the slow trials and vice versa to ensure that there was no difference in gap-onset times between slow and fast trials. The pupil size of the averaged slow versus fast trials was compared using a one-sample t test per time point. To account for multiple comparisons, p values were corrected across time points using a false discovery rate (FDR) of $q = 5\%$ (Benjamini and Hochberg, 1995).

MEG recording and preprocessing. MEG data were recorded using a CTF-MEG with 275 axial gradiometers at a sampling frequency of 1,200 Hz.

MEG data analysis was performed with the FieldTrip MATLAB toolbox (2019-09-20; Oostenveld et al., 2011). To avoid numerical issues during processing due to very small numbers associated with MEG recordings in the Tesla range, we multiplied all MEG data with 10^{12}, leading to data in the picotesla range. Data were filtered with a 100 Hz low-pass (Hann window, 89 points), a 0.7 Hz high-pass (Hann window, 2,869 points), and a 60 Hz elliptic band-stop filter to suppress line noise. Data were cut into 10.2 s trials ranging from −3 to 7.2 s time-locked to the noise onset. For the calculation of independent component analysis (ICA), these trials were divided into 1 s snippets. Components containing blinks, lateral eye movement, and heart-related activity were identified through visual inspection. The continuous data (filtered) were projected to ICA space using the unmixing matrix. The previously identified components containing artifacts were removed from the continuous data, and the data were then back-projected to the original 275 sensors using the mixing matrix. Data were then low-pass filtered at 30 Hz (Hann window, 111 points) and divided into trials of 10.2 s (−3 to 7.2 s time-locked to the noise onset). Data were downsampled to 600 Hz, and trials that exceeded a signal change of >4 picotesla in any of the MEG channels were excluded from analysis.

Analysis of event-related fields for the gap onset and button response. Data were transformed from axial to planar gradiometers (Vrba and Robinson, 2001). Planar gradiometers show the strongest sensitivity to sources that originate from directly below them (Hämäläinen, 1995; Vrba and Robinson, 2001), which makes the interpretation of topographical distributions more intuitive. The signal at the two planar gradiometers forming one pair was combined by calculating the sum. This resulted in signals at 275 sensors.

For the analysis of event-related fields (ERFs), we focused on hit trials, and each trial was time-locked to the respective gap-onset time. To investigate evoked auditory sensory processing, data were averaged across temporal sensors (MRF67, MRT13, MRT14, MRT15, MRT23, MRT24, MRT25, MRT2, MRT35, MRT36, MLF67, MLT13, MLT14, MLT15, MLT23, MLT24, MLT25, MLT26, MLT35, MLT36). For illustrative purposes, trials were averaged separately for each of the four conditions and baseline-corrected by subtracting the mean amplitude in the time window before the gap onset (−0.5–0 s) from each time point. For the statistical analysis, data were averaged across the time window of the M100 component of the ERF (0.09–0.13 s; Näätänen and Picton, 1987). The M100 time window was selected to investigate possible reward-prospect influences on auditory sensory processing.

For an exploratory analysis of the late ERF component with a parietal topography (Fig. 4*A*,*C*), hit trials were time-locked to a person's response time in the respective trial and averaged across parietal sensors (MLC16, MLC17, MLC24, MLC25, MLC31, MLC32, MLC41, MLC42, MLC53, MLC54, MLC55, MLC61, MLC62, MLC63, MRC16, MRC17, MRC24, MRC25, MRC31, MRC32, MRC41, MRC42, MRC53, MRC54, MRC55, MRC61, MRC62, MRC63, MLP11, MLP12, MLP21, MLP22, MLP23, MLP31, MLP32, MLP33, MLP34, MLP35, MLP41, MLP42, MLP43, MLP44, MLP45, MLP54, MLP55, MLP56, MLP57, MRP11, MRP12, MRP21, MRP22, MRP23, MRP31, MRP32, MRP33, MRP34, MRP35, MRP41, MRP42, MRP43, MRP44, MRP45, MRP54, MRP55, MRP56, MRP57, MZC03, MZC04, MZP01). For illustrative purposes, data were baseline-corrected using the same time window as for the gap-locked data (−0.5–0 s time-locked to the gap onset). For statistical analysis, single-trial response–locked data were averaged across the 0.1–0.6 s time window (time-locked to button response) to investigate task difficulty and reward-prospect effects on the response-related component (Fig. 4*D*).

Analysis of time–frequency power. In order to analyze oscillatory activity in the alpha frequency range (8 to 12 Hz; Klimesch et al., 2007; Jensen and Mazaheri, 2010; Weisz et al., 2011), single-trial time–domain data (after planar gradiometer calculation) were convolved with Morlet wavelets. Complex wavelet coefficients were calculated for frequencies ranging from 8 to 12 Hz (1 Hz steps) and time points ranging from –2 to 6.2 s (0.04 s steps) time-locked to the noise onset, separately for each trial, sensor, and participant. For the visualization of time–frequency data across a wider frequency range, calculations were also done for frequencies ranging from 1 to 20 Hz in steps of 1 Hz and in time steps of 0.16 s. We analyzed data first time-locked to the noise onset and then time-locked to the gap onset.

For the analysis of data time-locked to the noise onset (Fig. 5), power was calculated by squaring the magnitude of the complex wavelet coefficients separately for each trial, sensor, and time–frequency bin. Data for the two corresponding planar gradiometers of a pair were combined by calculating the sum, which resulted in power data for 275 sensors. For visualization purposes, time–frequency power per condition was averaged across trials and baseline-corrected to decibel power change: data at each time point were divided by the mean power in the baseline time window (−1.5 to −1.1 time-locked to the noise onset) and subsequently log10 transformed. To visualize the difference in power between hit and miss trials, we categorized trials as hit and miss trials and averaged them across parietal sensors. For statistical analysis, parietal alpha power in the 1.7 to 2.2 s time window (time-locked to the noise onset) was averaged. This time window was chosen because it precedes the time window during which a gap could occur (2.2–4.2 s).

For the investigation of alpha activity changes related to gap detection, we time-locked the data to the gap onset and focused on hit trials only. This was done on single-trial complex wavelet coefficients, and power calculation and gradiometer combination were performed in the same way as for the noise-locked data above. For visualization purposes, condition-averaged data were baseline-corrected to decibel power change using the same time window as for the noise-locked data (−1.5 to −1.1 s time-locked to the noise onset) and separately averaged across parietal or temporal sensors (see section above). For the statistical analysis, pregap alpha power for each trial was averaged across the −0.5–0 s time window (time-locked to the gap onset).

Trials in which participants detected the gap elicited an alpha-power suppression (Fig. 5*D*). We thus also investigated possible effects of task difficulty and reward prospect on the postgap alpha-power suppression. To this end, we calculated the latency of minimal alpha power between 0 and 1 s postgap for each condition and participant. For the statistical analysis of the alpha power at its minimum, we averaged the data ±40 ms around the estimated latency for each trial.

Source localization. For source localization, the MRI image of the standard brain and skull in FieldTrip toolbox was nonlinearly warped for each participant to fit their head shape data from the Polhemus digitization. An automatic FreeSurfer's approach was used to segment the MRI and extract the cortical mesh. This procedure ensured that the cortical mesh consisted of comparable grid-point locations across participants (Alavash et al., 2021) in accordance with the Human Connectome Project (HCP) standard atlas template (Keitel and Gross, 2016; Glasser et al., 2017). This cortical mesh served as the source model for each participant. FieldTrip's "singleshell" method was used to calculate the inner skull surface that was used as a volume conductor model. Subsequently, leadfields were calculated separately for each experimental block to account for the slightly different head positions relative to the sensors in the different MEG recording blocks.

For each participant and block, a multitaper (±2 Hz spectral smoothing) fast Fourier transform (FFT) was calculated. The complex coefficients at 10 Hz that resulted from the FFT were used to calculate a cross-spectral density matrix per block. Dynamic imaging of coherent sources was used for source localization (Gross et al., 2001). For each source location, a spatial filter was calculated using a participant's cross-spectral density matrix (dipole orientation, axis of most variance using singular value decomposition). For each trial, spatial filter weights were multiplied time point per time point with the complex wavelet coefficients from the analysis that used data time-locked to the gap onset (8–12 Hz frequency range). Power was calculated by squaring the magnitude of the complex wavelet coefficients that were projected through the spatial filter. Time–frequency source power was averaged across the 8–12 Hz frequencies.

For the statistical analysis, we focused on two predefined regions of interest (ROIs) according to functional parcels defined by the Glasser atlas as available in the HCP workspace (Keitel and Gross, 2016;

Glasser et al., 2017). We included an auditory ROI due to the auditory nature of the task and because auditory stimulation is known to elicit sensory alpha activity (Mazaheri et al., 2014; Wöstmann et al., 2017; Herrmann et al., 2023; Kraus et al., 2023b). We also included a parietal ROI, because the parietal cortex is part of the attentional networks and is known to elicit alpha activity under task load (Rushworth et al., 2001; Behrmann et al., 2004; Banerjee et al., 2011; Herrmann et al., 2023; Kraus et al., 2023b). To analyze postgap alpha-power suppression in source space, we calculated the latency of minimal alpha power between 0 and 1 s postgap per condition, participant, and ROI. For each trial, we then averaged the data ±40 ms around the estimated latency.

For visualization only, hit trials were averaged for each condition and participant. The decibel power change was calculated relative to the original baseline time window (−1.5 to −1.1 s time-locked to the noise onset).

Statistical analysis. A paired sample *t* test was used to analyze the subjective rating of cue use. The effect size was reported as Cohen's *d* (J. Cohen, 1988).

A variety of linear mixed-effect models (LMMs) in R (v4.1.2), with the packages lme4 and sjPlot, were used for the statistical analyses. All LMMs included participant-specific random intercepts to account for individual differences in the respective dependent variable. Single-trial accuracy data were binary. Hence, for accuracy data, a generalized LMM (GLMM) with a binomial distribution and a logit link function was used (Tune et al., 2021; Kraus et al., 2023a). All other models included continuous data as dependent variables, and we thus used an LMM with a Gaussian distribution and an identity link function (Tune et al., 2021; Kraus et al., 2023a). All continuous variables were *z*-scored. All models predicting behavioral outcomes included the gap time as a regressor to account for hazard-rate effects (Niemi and Näätänen, 1981; Nobre et al., 2007; Herrmann et al., 2023). For all statistical models using neurophysiological data as dependent variable, data averaged across the baseline time window were included in the model as a separate regressor instead of using baseline-corrected data as the dependent variable (Alday, 2019).

First, LMMs were calculated to analyze the influence of the two experimental factors on behavioral outcomes, pupil size, M100 component, and alpha power. The models included effects of task difficulty (easy, hard), reward prospect (reward-irrelevant, reward-relevant), and task difficulty × reward prospect interaction. Task difficulty and reward prospect were categorical predictors and were, therefore, deviation-coded [i.e., −0.5 (easy, no-reward) and 0.5 (hard, reward)].

Second, LMMs were calculated to analyze the influence of the pupil size or parietal alpha power on accuracy or response time. For these analyses, only hard trials were used because of the large variance in the behavioral measures between easy and hard conditions and the ceiling performance for the easy condition. The pupil size and parietal alpha power were used as independent variables in these models; therefore, baseline correction was needed before inclusion into the respective statistical model. Including the baseline data as an additional regressor (as described for the prediction of pupil/alpha data) would lead to collinearity issues. For pupil size data, we used subtractive baselining (see above, Pupil data recording and preprocessing), which can be used on single trials (Mathôt et al., 2018). However, decibel power baselining should not be used on single-trial data (M. X. Cohen, 2014). To account for this, we calculated a model with pregap alpha power as the dependent variable and alpha power within the baseline time window as the only independent variable. The residuals of this model served as the alpha-power regressor in the models to predict behavioral outcomes (Alday, 2019).

To disentangle associations of the pupil size/alpha power and behavior at the trial-by-trial state level (i.e., within-participant) from associations at the trait level (i.e., between-participants), we included two separate regressors associated with changes in the pupil size/alpha power. The between-participant regressor contained trial-averaged pupil size/alpha power per individual, whereas the within-participant regressor contained the single-trial pupil size/alpha power relative to the individual mean (Bell et al., 2019; Tune et al., 2021; Kraus et al., 2023a, b). Reward prospect and gap time were included as regressors to account for their potential influence on behavior. A random slope for the within-participant effect was included whenever it improved the respective model and did not lead to missing convergence of the model.

Third, an LMM was calculated to analyze the relationship between the M100 amplitude and the postgap alpha power. Reward prospect, task difficulty, and their interaction were included as regressors to account for their potential influence on postgap alpha power. A within-participant and a between-participant regressor were included for the M100 amplitude regressor as well as a random slope for the within-participant effect.

Fourth, LMMs were calculated to analyze the relationship between the pregap pupil size and the M100 amplitude or the postgap alpha power. Reward prospect, task difficulty, and their interaction were included as regressors to account for their potential influence on the M100 amplitude or postgap alpha power. A within-participant and a between-participants regressor were included for the pupil size regressor, as well as a random slope for the within-participant.

For the interpretation of effects analyzed with the different LMMs, we calculated Bayes factors (BFs) as $\log(BF) = [BIC(H0) - BIC(H1)] / 2$, with BIC being the Bayes–Schwartz information criterion (Wagenmakers, 2007; Alavash and Obleser, 2024). To this end, we calculated the BIC for the full model, including the regressor of interest (H1), and for the reduced model, excluding the regressor of interest (H0). A log(BF) larger than 1 provides evidence for the presence of an effect of the regressor of interest, whereas a log(BF) value smaller than –1 suggests the absence of an effect of the regressor of interest (Dienes, 2014).

Data availability. All data and analysis scripts are available at https://osf.io/prwb7/.

Results

Reward prospect improves performance

As intended, performance was better in the easy compared with that in the hard condition for both accuracy and response time [accuracy, GLMM; odds ratio (OR) = 0.05; standard error (SE) = 0.004; $p = 1.74 \times 10^{-238}$; log(BF) = Inf; response time, LMM; $\beta = 0.35$; SE = 0.007; $p < 1.74 \times 10^{-238}$; log(BF) = Inf; Fig. 2]. Furthermore, participants were more accurate and faster for the reward-relevant compared with the reward-irrelevant condition [accuracy, OR = 1.31; SE = 0.117; $p = 3.54 \times 10^{-3}$; log(BF) = −0.15; response time, $\beta = -0.03$; SE = 0.007; $p = 8.87 \times 10^{-5}$; log(BF) = 3.35]. The interaction was not significant [accuracy, OR = 0.98; SE = 0.175; $p > 0.9$; log(BF) = −4.6; response time, $\beta = -0.02$; SE = 0.014; $p > 0.2$, log(BF) = −3.75]. We found a hazard-rate effect, such that individuals were more accurate and faster when the gap occurred later rather than earlier [accuracy, OR = 1.21; SE = 0.036; $p = 3.19 \times 10^{-10}$; log(BF) = 15.8; response time, $\beta = -0.08$; SE = 0.003; $p = 2.44 \times 10^{-118}$; log(BF) = 263.5].

Participants rated their use of the auditory cue to distinguish between reward-relevant and reward-irrelevant higher in the hard compared with the easy condition ($t_{(36)} = 3.54$; $p = 1.11 \times 10^{-3}$; $d = 0.58$).

Reward prospect modulates the task difficulty effect on the pupil size

To investigate the influence of task difficulty and reward prospect on the pupil size, we averaged the pupil size over the time window ranging from 2.2 to 6.2 s (Fig. 3*B*; time-locked to the noise onset). The pupil size was larger for hard compared with easy trials [$\beta = 0.05$; SE = 0.009; $p = 5.21 \times 10^{-7}$; log(BF) = 9.1] and larger for reward-relevant compared with reward-irrelevant trials [$\beta = 0.03$; SE = 0.009; $p = 3.32 \times 10^{-4}$; log(BF) = 2.6]. Importantly, we observed a significant task difficulty × reward prospect interaction, indicating a larger increase in the pupil size for

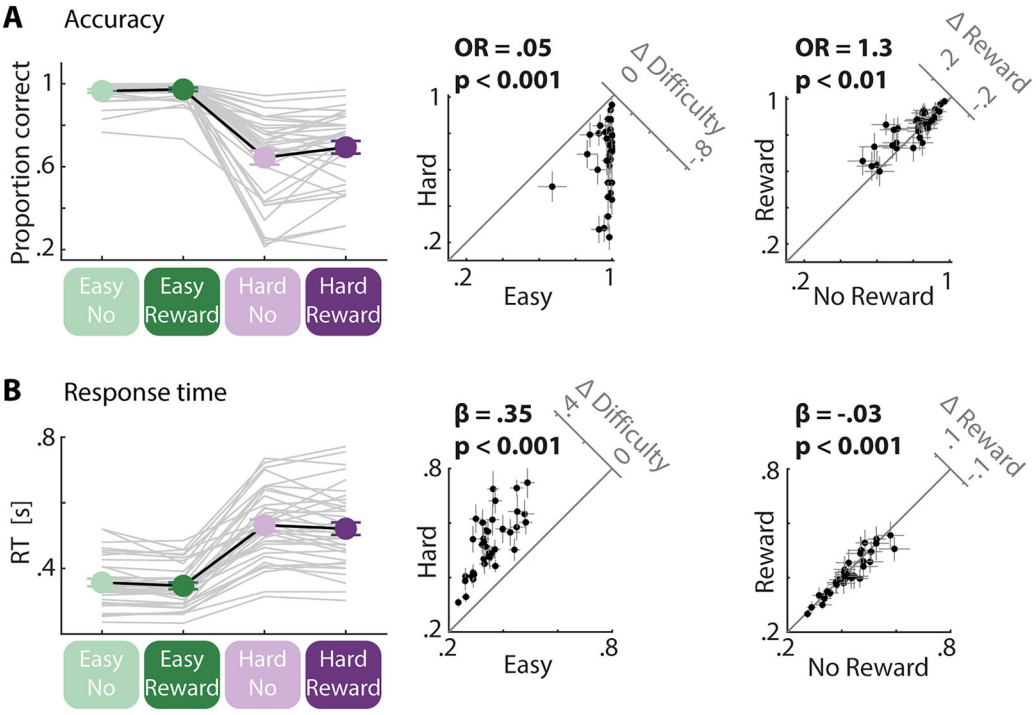

Figure 2. Behavioral results. ***A***, Accuracy. Proportion correct was better for the easy compared with the hard condition and for the reward-relevant compared with the reward-irrelevant condition. Insets, 45° scatterplots showing the task difficulty (left) and the reward-prospect effect (right) from linear mixed-model analysis. Difference plots (*y*- minus *x*-axis) are shown in the top-right corners). ***B***, Response time. Participants were faster for the easy compared with the hard condition and for the reward-relevant compared with the reward-irrelevant condition. Insets, 45° scatterplots showing the task difficulty (left) and the reward-prospect effect (right) from linear mixed-model analysis. Difference plots (*y*- minus *x*-axis) are shown in the top-right corners.

reward-relevant than reward-irrelevant trials when task difficulty was hard compared with easy [$\beta = 0.04$; SE = 0.018; $p = 3.08 \times 10^{-2}$; log(BF) = −1.9; Fig. 3*C*].

Next, we investigated whether a larger pupil size during the interval preceding the gap is associated with behavioral performance. This analysis was conducted using the hard trials only, and the information about the reward conditions was included as a regressor into the model. With this approach we controlled for the effects of reward prospect and task difficulty on both the pupil size and response time. To this end, pupil size data for hard trials were aligned to gap-onset times, and the pupil size was averaged across the −0.5–0 s pregap time window. The pregap pupil size did not predict behavioral accuracy, neither at the trial-by-trial state level [within-participant, OR = 1.07; SE = 0.043; $p > 0.1$; log(BF) = −2.7] nor at the trait level [between-participants: OR = 1.04, SE = 0.158, $p > 0.8$, log(BF) = −1.6]. However, at the trial-by-trial state level, response times were shorter when the pregap pupil size was larger [within-participant, $\beta = -0.02$; SE = 0.008; $p = 9.03 \times 10^{-3}$; log(BF) = 0], but at the trait level there was no association between a participant's mean pupil size and mean response time [between-participants, $\beta = -0.01$; SE = 0.038; $p > 0.8$; log(BF) = −1.6; Fig. 3*F*]. To illustrate this effect, we grouped the hard trials into fast- and slow-response trials, separately for the reward-relevant and the reward-irrelevant condition (trials were selected such that the mean gap time for fast- and slow-response trials did not differ; see Materials and Methods). The pupil size was significantly larger for fast trials compared with that for slow trials already >1 s before the gap onset (Fig. 3*E*).

In addition, we conducted a temporal response function (TRF) analysis (Crosse et al., 2016) to ensure that the observed interaction of task difficulty and reward prospect is not resulting from a temporal shift in the pupil size response due to response-time differences between conditions (Fig. 2*B*). The time points of the noise onset, gap onset, and response time of the respective trial served as separate regressors to model the TRFs to the different events. The TRF to the gap onset (Fig. 3*G*, left) but not to the button response (Fig. 3*G*, right) shows temporal variability between the different experimental conditions. However, importantly, we observed the interaction of task difficulty and reward for both the TRF to gap onset (1.82 to 2.56 s) and to the button response (1.38 to 2.22 s). Additionally, the pupil size TRF was larger for hard compared with easy trials (TRF to the gap onset, −2 to −0.88 s and 1.36–3.14 s; TRF to button response, 0.96–2.54 s).

Task difficulty, but not reward prospect, affects the auditory sensory response

We tested whether task difficulty and reward prospect influenced sensory responses, that is, responses in the auditory cortex. To this end, we focused on the M100 component in the 0.09–0.13 s time window after the gap onset in temporal sensors. The M100 amplitude was larger for easy (i.e., longer gap duration) compared with hard trials [i.e., shorter gap duration; $\beta = -0.40$; SE = 0.013; $p = 1.33 \times 10^{-200}$; log(BF) = 210.5; Fig. 4*A*,*B*]. The effect for reward prospect [$\beta = -0.00$; SE = 0.017; $p > 0.9$; log(BF) = −4.5] and the interaction were not significant [$\beta = -0.01$; SE = 0.034; $p > 0.9$; log(BF) = −4.5].

Task difficulty and reward prospect modulate the response-related evoked field

We also explored the late ERF component from 0.5 s onward (Fig. 4*A*). Because the topography indicates the responses originate from the parietal cortex, the analysis of this component focused on parietal sensors. Sorting the gap-locked trials

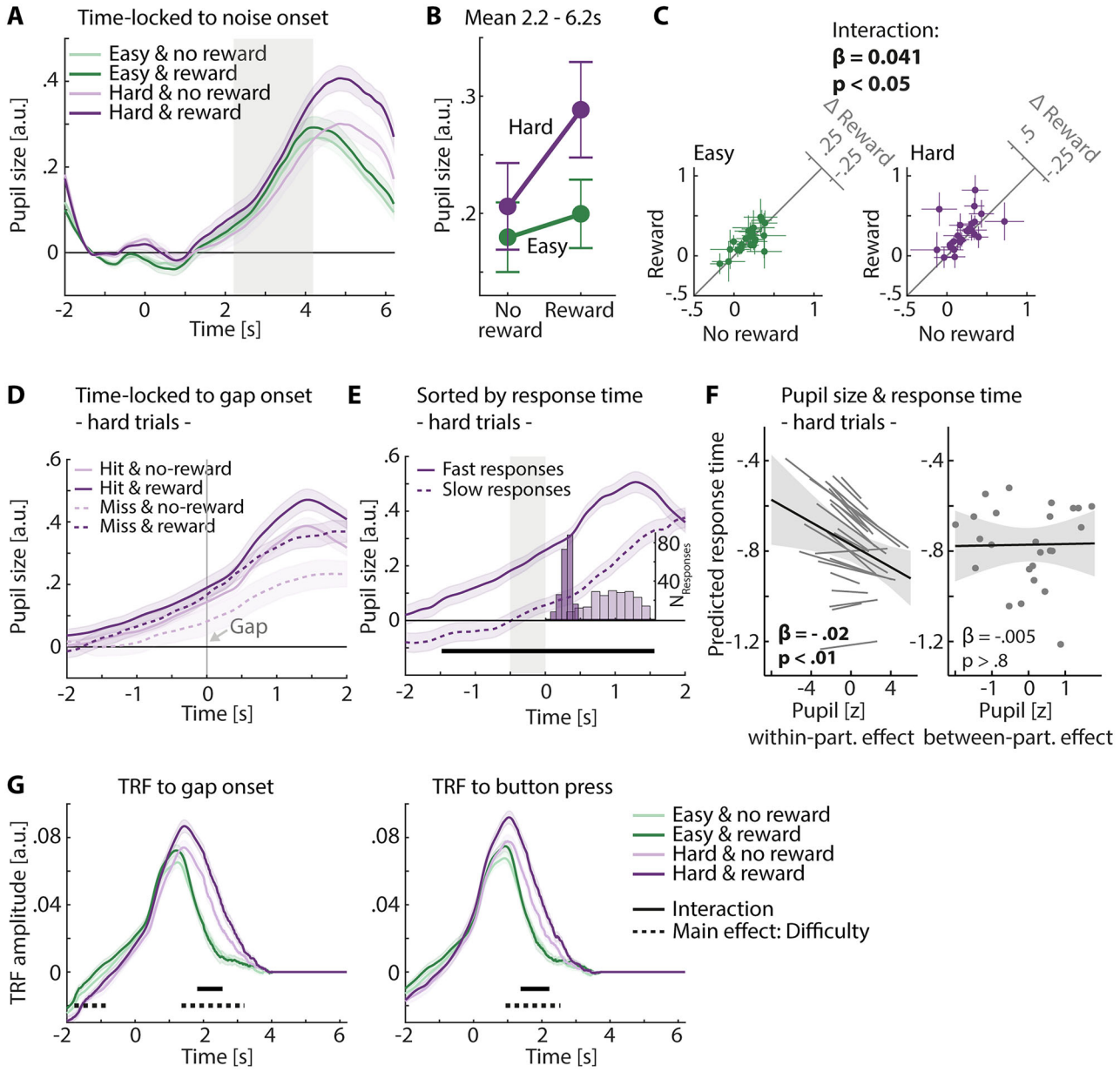

Figure 3. Pupil size results. ***A***, Averaged pupil size time courses across participants per condition. Error bands reflect the within-participant error. Gray areas indicate time window during which a gap could occur, from 2.2 to 4.2 s. ***B***, Averaged data for 2.2–6.2 s time window. Error bars indicate the standard error of the mean. ***C***, 45° scatterplots illustrate the interaction. Left, Data from the easy condition. Right, Data from the hard condition. Colored dots show averaged pupil data per task difficulty level, separately for each participant. The 45° line indicates no difference between conditions. Crosshairs indicate the 95% confidence interval. Difference plots (*y*- minus *x*-axis) are shown in top-right corners. ***D***, Pupil size time courses (time-locked to the gap onset) for the hard condition, separately for each reward-prospect condition (light vs dark) and for hit and miss trials (solid vs dashed lines). Error bands reflect the within-participant error. ***E***, Pupil size data grouped into trials with slow- (dashed) and fast-response times (solid). The histogram shows the distribution of response times for each group. Gray area indicates the time window for the LMM analysis in panel ***F***. Black line indicates the time window in which the pupil size was significantly larger for fast-response trials compared with slow-response trials (after FDR correction). Error bands reflect the within-participant error. ***F***, Effect of the pupil size on response time in an LMM analysis. A larger pupil size is associated with a faster response time on a within-participant level (not for the between-participants effect). Participant-specific slope for the pupil size did not improve the model, but we show it here for illustrative purposes. ***G***, TRF approach of the pupil size response to the gap onset (left) and button press (right). Black line indicates the time window in which the pupil size increased stronger for reward-relevant than reward-irrelevant trials when task difficulty was hard compared with easy. Dashed black line indicates the time window in which the pupil size was significantly larger in hard compared with easy trials. All shown significant effects are based on FDR correction.

according to their response times (Fig. 4*C*) shows that this component is time-locked to the response rather than to the gap onset (at 0 s in Fig. 4*C*), because the negative deflection succeeds the response time (dashed line). Hence, we analyzed this component time-locked to the button response (Fig. 4*D*) instead of time-locked to the gap onset. Topographies for the time windows before, during, and after the button response are shown in Figure 4, *D* and *E*, indicating that the response-related component is similar to the component we observed in the gap-locked analysis (Fig. 4*C*). The response-related component was stronger deflected for hard than easy trials [$\beta = -0.18$; SE = 0.013; $p = 1.54 \times 10^{-39}$; log(BF) = 83] and for reward-relevant than reward-irrelevant trials [$\beta = -0.04$; SE = 0.013; $p = 1.33 \times 10^{-3}$; log(BF) = 1; Fig. 4*E*]. The interaction was not significant [$\beta = -0.05$; SE = 0.026; $p > 0.05$; log(BF) = −2.5].

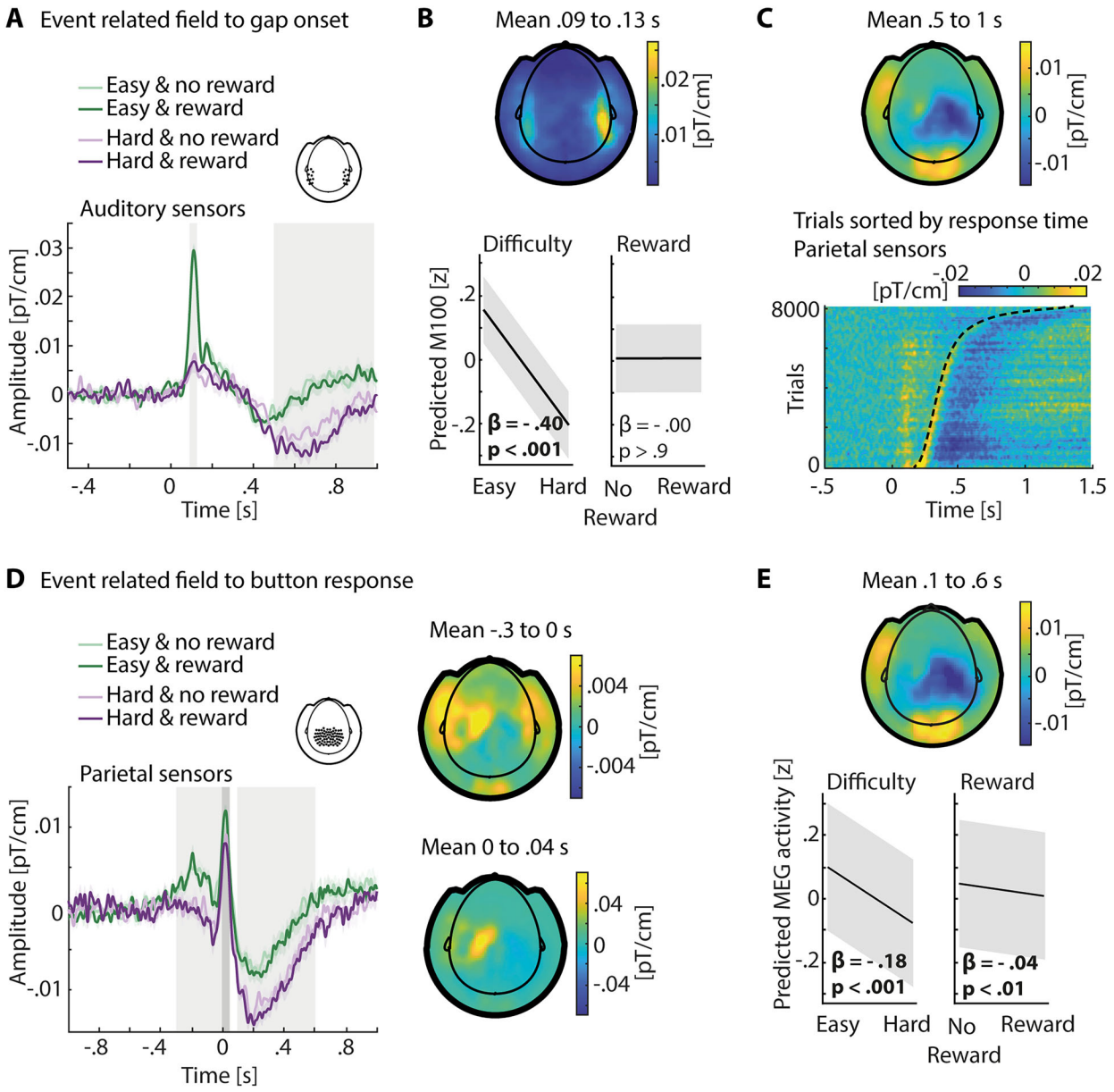

Figure 4. Event-related field to the gap onset and to the button response. ***A***, Event-related field to the gap onset. Data are averaged across temporal sensors marked in the inset. Error bands reflect the within-participant error. Gray areas indicate time windows for analysis in ***B*** and ***C***. ***B***, Effect on M100. Average from 0.09 to 0.13 s. Top, Topography for the average across all for conditions. Bottom, Statistical results are calculated using an LMM. Main effect is significant for difficulty but not for reward prospect. ***C***, Late ERF component. Top, Topography for the average across all four conditions from 0.5 to 1 s. Bottom, Trials sorted by response time and time-locked to the gap onset. Average across parietal sensors that are marked in the inset in panel ***D***. Data are from all conditions. Black dashed line indicates response time. ***D***, Event-related field to button response. Data are averaged across parietal sensors marked in the inset. Error bands reflect the within-participant error. Gray areas indicate time windows for topographies on the right and in panel ***E***. Topographies for time window before button response and around button response show main activity around left motor areas. ***E***, After-response component. Top, Topography for the average across all four conditions from 0.1 to 0.6 s. Bottom, Statistical analysis of time window 0.1–0.6 s after button response using an LMM. Stronger deflection for hard compared with easy trials and for reward-relevant compared with reward-irrelevant trials. All significant effects are based on FDR correction.

Neither reward prospect nor task difficulty modulate pregap parietal alpha power

The time–frequency analysis shows that parietal alpha power in the 8–12 Hz frequency band increased over time after the noise onset, up to when the gap occurred (Fig. 5*C*). However, alpha power in the 1.7 to 2.2 s time window after the noise onset (i.e., 0.5 s before any gap could occur) showed no effect of task difficulty [$\beta = 0.00$; SE = 0.016; $p > 0.9$; log(BF) = −4.5], reward prospect [$\beta = -0.01$; SE = 0.016; $p > 0.9$; log(BF) = −4.5], nor the interaction [$\beta = -0.02$; SE = 0.032; $p > 0.9$; log(BF) = −4.5]. Grouping trials according to hits and misses (irrespective of condition) showed the pregap alpha power increase for hits but not for miss trials. For hit trials, alpha power also decreased after the gap onset (Fig. 5*D*).

Alpha-power time courses were time-locked to the gap onset for an analysis of the exact time window before the gap onset. We investigated whether alpha power in the pregap time window (−0.5 to 0 s) was affected by our experimental manipulations. However, neither the effect of reward prospect [$\beta = -0.01$; SE = 0.016; $p > 0.5$; log(BF) = −4.5], task difficulty [$\beta = -0.02$; SE = 0.016; $p > 0.5$; log(BF) = −4], nor the interaction were significant [$\beta = -0.03$; SE = 0.032; $p > 0.5$; log(BF) = −4.5].

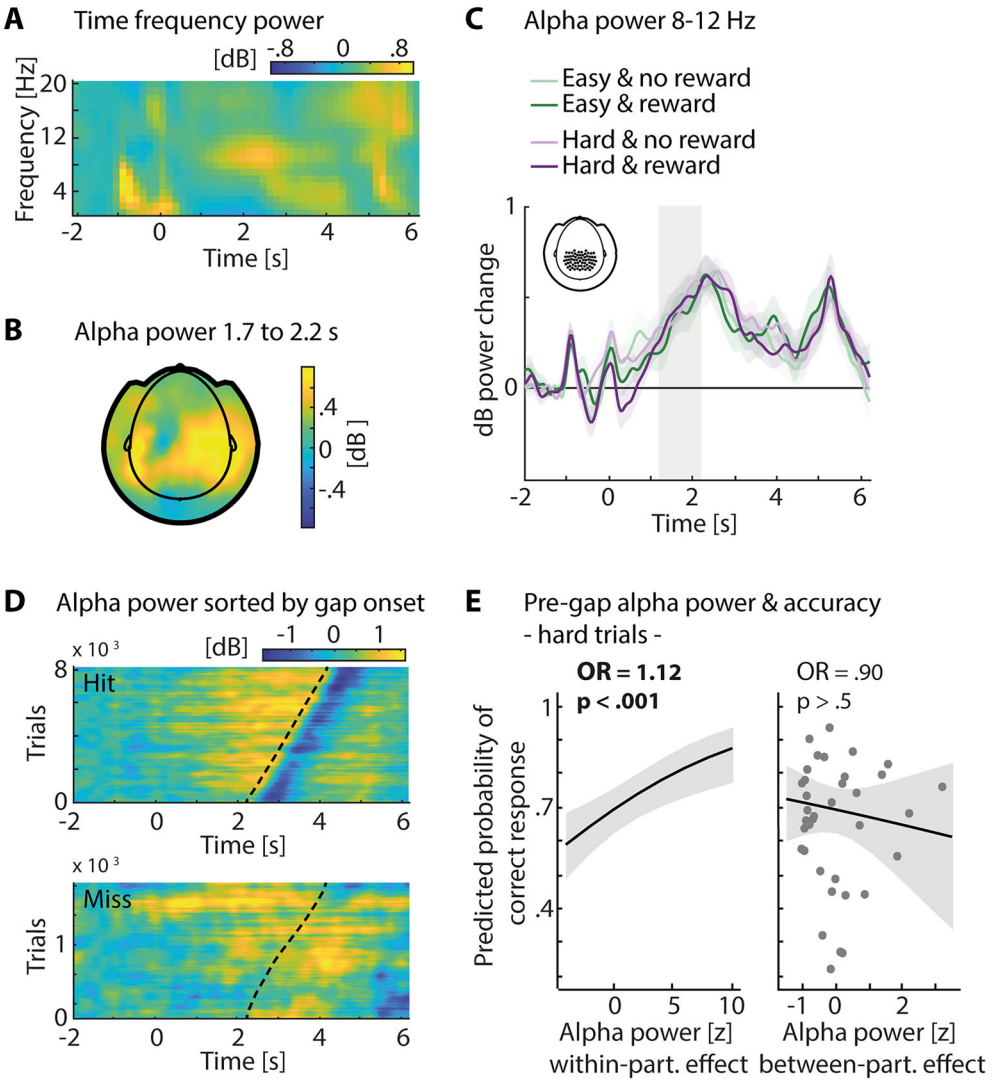

Figure 5. Pregap alpha-power analysis. All data are averaged across parietal sensors marked in the inset in panel ***C***. ***A***, Time–frequency power measured in decibel relative to a prestimulus time interval and averaged across all conditions. ***B***, Topography reflects alpha power in the 500 ms (1.7–2.2 s) before the time window when a gap could occur (averaged across all conditions; gray area in ***C***). ***C***, Alpha power averaged for all four conditions separately. Error bands reflect the within-participant error. Effects of task difficulty and reward prospect were not significant in the 500 ms before a gap could occur (gray area). ***D***, Alpha power for hit trials (top) and miss trials (bottom) sorted by the gap onset. Black dashed lines indicate the gap time. Alpha power increased toward the gap but was suppressed after gap occurrence (for hit trials). ***E***, Effect of pregap parietal alpha power on accuracy in an LMM analysis. Larger pregap alpha power is associated with better performance on a within-participant level only. Reported effects are based on FDR correction.

Although pregap alpha power was not modulated by task difficulty or reward prospect, we found a positive correlation between pregap alpha power and behavior. The probability of detecting a gap (for hard trials) was higher when pregap alpha power in parietal sensors was larger (Fig. 5*E*). This effect was present on the within-participant level [OR = 1.12; SE = 0.037; $p = 7.81 \times 10^{-4}$; log(BF) = 1.7], but not on the between-participants level [OR = 0.90; SE = 0.143; $p > 0.5$; log(BF) = −1.6]. There were no significant alpha-power effects on response time [within-participant, $\beta = 0.03$; SE = 0.029; $p > 0.2$; log(BF) = −3.5; between-participants, $\beta = 0.19$; SE = 0.142; $p > 0.2$; log(BF) = −1.1].

Reward prospect modulates postgap alpha-power suppression

We further explored the alpha-power suppression that followed the gap. Figure 6*A* suggests the alpha suppression is related to the gap rather than the button press, as illustrated by relation of the two dashed lines to the alpha-power suppression in Figure 6*A*. Task difficulty led to a postgap alpha-power suppression that was only marginally significant for temporal sensors [$\beta = -0.04$; SE = 0.018; $p = 4.03 \times 10^{-2}$; log(BF) = −2; Fig. 6*C*] and not significant for parietal sensors ($\beta = -0.03$, SE = 0.018, $p > 0.2$, log(BF) = −3.5, Fig. 6*D*). However, alpha power was more suppressed in reward-relevant compared with reward-irrelevant trials for temporal sensors [$\beta = -0.07$; SE = 0.017; $p = 3.33 \times 10^{-4}$; log(BF) = 3] and parietal sensors [$\beta = -0.05$; SE = 0.018; $p = 1.53 \times 10^{-2}$; log(BF) = −0.5]. For neither of the two sensor clusters the interaction was significant [temporal sensors, $\beta = -0.06$; SE = 0.035; $p > 0.1$; log(BF) = −3; parietal sensors, $\beta = -0.03$; SE = 0.036; $p > 0.4$; log(BF) = −4]. Projecting gap-locked alpha–power data into source space revealed qualitatively similar results to the results in sensor space, although not all effects reached statistical significance in source space (Fig. 7).

Correlating the M100 amplitude with the postgap alpha-power suppression revealed a positive relationship. When the M100 amplitude across temporal sensors was enhanced, subsequent alpha power was less suppressed in both temporal [within-participant, $\beta = 0.11$; SE = 0.020; $p = 2.74 \times 10^{-8}$; log(BF) = 108;

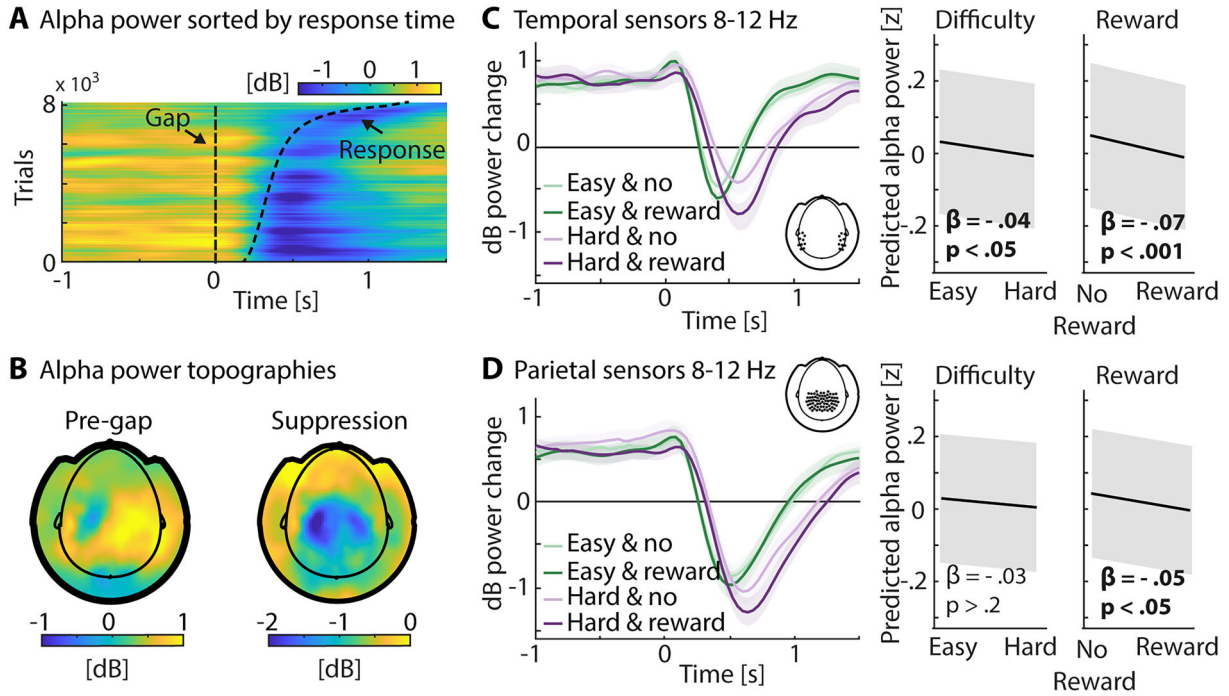

Figure 6. Postgap alpha-power analysis. ***A***, Gap-locked alpha–power trials sorted by response time. Data are averaged across parietal sensors; see inset in ***D***. Black lines represent the gap onset and the response time. Alpha-power suppression is rather time-locked to the gap onset than to the response time. ***B***, Left, Grand average topography for −0.5–0 s time-locked to the gap onset. Right, Grand average topography for maximal alpha-power suppression after the gap onset. ***C***, Temporal sensors. Left, Alpha power averaged per condition across participants and temporal sensors (see inset). Error bands reflect the within-participant error. Right, LMM results of alpha-power suppression. Alpha-power suppression was larger for hard compared with easy and for reward-relevant compared with reward-irrelevant trials. ***D***, Parietal sensors. Left, Alpha power averaged per condition across participants and parietal sensors (see inset). Error bands reflect the within-participant error. Right, LMM results of alpha-power suppression. Alpha-power suppression was larger for reward-relevant compared with reward-irrelevant trials.

between-participants, $\beta = 0.37$; SE = 0.049; $p = 6.26 \times 10^{-13}$; log(BF) = 12.8] and parietal sensors [within-participant, $\beta = 0.09$; SE = 0.016; $p = 2.74 \times 10^{-8}$; log(BF) = 47; between-participants, $\beta = 0.20$; SE = 0.076; $p = 1.36 \times 10^{-2}$; log(BF) = 1.2].

Larger pregap pupil size covaries with lower pregap parietal alpha power

To investigate the relationship between pupil size and brain measures, we calculated different LMMs (Fig. 8). First, we tested whether the pregap pupil size is associated with auditory cortex responses to the gap (M100 amplitude; averaged across temporal sensors). There was no within-participant effect [$\beta = -0.01$; SE = 0.018; $p > 0.6$; log(BF) = −6] nor a between-participants effect [$\beta = -0.07$; SE = 0.053; $p > 0.4$; log(BF) = −1.73].

Second, we investigated whether the pregap pupil size is associated with pregap parietal alpha power (averaged across parietal sensors). A larger pupil size was associated with lower parietal alpha power on a within-participant level [$\beta = -0.05$; SE = 0.02; $p = 1.25 \times 10^{-2}$; log(BF) = 5.5; Fig. 8*B*]. There was no significant effect on a between-participant level [$\beta = -0.06$; SE = 0.104; $p > 0.6$; log(BF) = −1.64]. Importantly, controlling for possible changes of alpha power over time via including the trial number across the experiment as an additional regressor into the model had no effect on the results.

Discussion

In the current study, we investigated a listener's motivation affecting behavior, pupil size, and neural activity during a challenging auditory detection task. Participants performed better, and the pupil size increased when listeners were more motivated compared with when they were less motivated by reward prospects. Neural oscillatory activity in parietal regions increased throughout the presentation of the noise sound, but this power increase was independent of task difficulty and reward prospect. Auditory sensory responses to auditory target stimuli were not modulated by reward prospect. However, both task difficulty and reward prospect independently enhanced postgap activity. In sum, pupil size changes index cognitive investment during the interplay of listening demand and motivation, whereas motivation impacts neural indices poststimulus rather than preparatory attentional modulation. The current study thus shows the complex and distinct impacts of motivation and listening demands on different neurophysiological systems.

Motivational state moderates the effect of listening demand on the pupil size

The pupil size increased as listening demands increased, as expected (Kahneman and Beatty, 1966; Zekveld et al., 2010; Koelewijn et al., 2012; Winn et al., 2015; Wendt et al., 2016; Ohlenforst et al., 2018; Kadem et al., 2020; Kraus et al., 2023b). Previous work has also shown that the pupil size is sensitive to individuals giving up listening under impossible listening conditions (Zekveld and Kramer, 2014; Ohlenforst et al., 2017; Herrmann and Ryan, 2024). The observation of the current study that a low motivational state is associated with a smaller pupil size, especially under high listening demands (Fig. 3*B*), is consistent with the literature on "giving up" listening. People may invest less cognitively when they are little motivated (Brehm and Self, 1989; Pichora-Fuller et al., 2016; Koelewijn et al., 2018; Herrmann and Johnsrude, 2020; Kraus et al., 2023a). A consideration in the current study may be that response times differed between conditions and that response time temporally

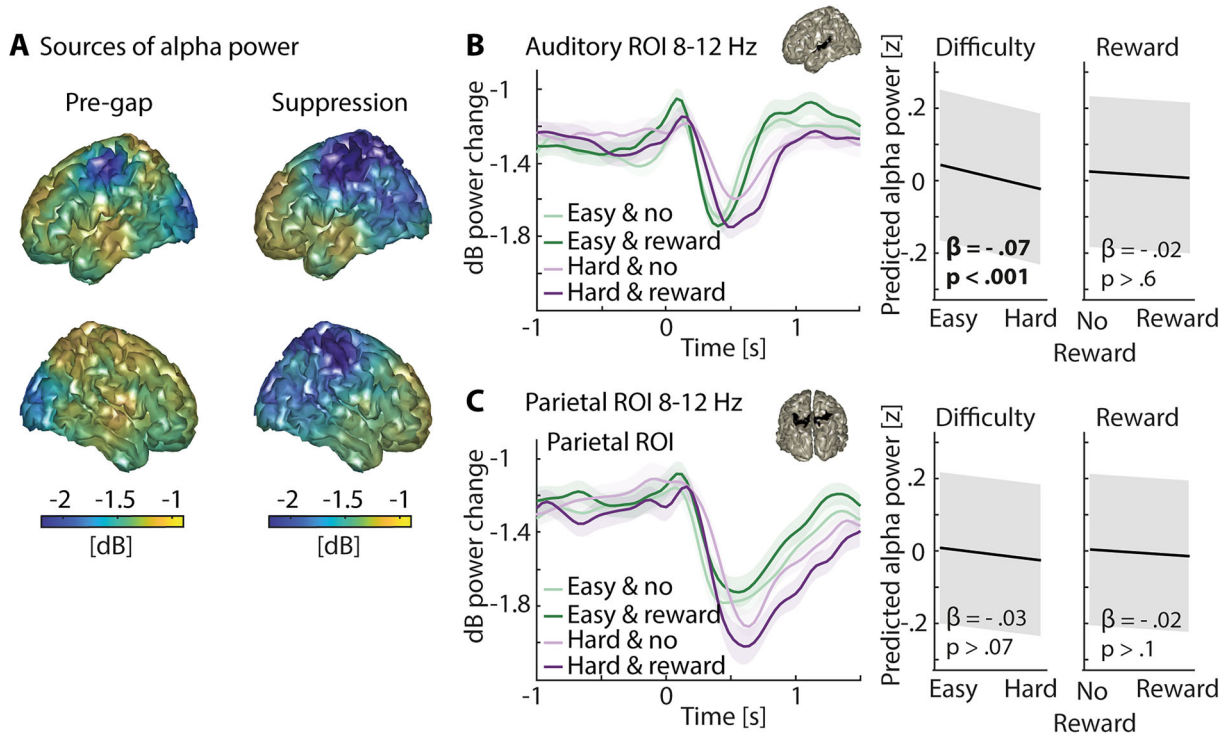

Figure 7. Source localized alpha power, time-locked to the gap onset. ***A***, Left, Grand average source plot for −0.5–0 s time-locked to the gap onset. Right, Grand average source plot for maximal alpha-power suppression after the gap onset. ***B***, Auditory ROI. Left, Source-projected alpha power for each condition. Inset shows the auditory ROI. Error bands reflect the within-participant error. Right, Results from an LMM predicting alpha-power suppression. Alpha-power suppression was larger for hard compared with easy trials [$\beta = -0.07$; SE = 0.018; $p = 9.64 \times 10^{-4}$; log(BF) = 2.5]. The effect of reward [$\beta = -0.02$; SE = 0.018; $p > 0.6$; log(BF) = −4] and the difficulty × reward interaction [$\beta = 0.02$; SE = 0.036; $p > 0.7$; log(BF) = −4.5] were not significant. Direction of the effects is the same as in sensor space. ***C***, Same as in panel ***B*** for a parietal ROI. No significant effect was found [task difficulty, $\beta = -0.03$; SE = 0.016; $p > 0.7$; log(BF) = −2.5; reward prospect, $\beta = -0.02$; SE = 0.016; $p > 0.1$; log(BF) = −3.5; interaction, $\beta = -0.06$; SE = 0.031; $p > 0.1$; log(BF) = −3]. Direction of the effects is the same as in sensor space.

aligned with the pupil dilation. However, the moderating effect of the motivational state on the task difficulty effect on the pupil size remains qualitatively the same when controlling for the potential confound of the different response times (Fig. 3*G*).

Critically, the behavioral results by themselves suggest that the influence of motivation is independent of the influence of listening demand (two main effects; Fig. 2). However, the pupil size results indicate, consistently with cognitive control frameworks (Brehm and Self, 1989; Parro et al., 2018; Yee and Braver, 2018), that motivation is most impactful under difficult compared with easy listening demands. Consequently, based on motivational intensity theory (Brehm and Self, 1989; Richter, 2016), the individual motivational state is another important determinant of the amount of effort allocated during listening besides the level of listening demand. The here and previously found increases in pupil size and response speed with heightened motivation (Kraus et al., 2023a) highlight the importance of taking listeners' motivation into account when assessing their invested effort. Our pupil size data thus provide an important confirmation to examine motivational impacts on the neural level.

Expectations about different levels of listening demand are not sufficient to modulate alpha power

Parietal alpha power increased throughout the presentation of the noise up to when individuals detected the gap (Fig. 5*C*). Alpha power thus showed sensitivity to when in time attention is allocated, followed by a poststimulus suppression (Herrmann et al., 2023). However, in contrast to previous work (Obleser et al., 2012; Petersen et al., 2015; Wöstmann et al., 2015; Wisniewski et al., 2017) and our hypothesis, we did not observe an increase in parietal alpha power with increasing task demand nor when listeners could expect a reward for performing well. One important difference between our and these former studies is that different tasks and time windows of interest were employed. Most of the studies that report demand-related effects on parietal alpha power during listening observed them in a memory task, during the retention period when participants held a stimulus in memory to compare it with a later probe stimulus (Obleser et al., 2012; Petersen et al., 2015; Wöstmann et al., 2015; Wisniewski et al., 2017). In the present study, we investigated alpha-power changes in a period—leading up to a behaviorally relevant auditory event—during which our experimental conditions were acoustically identical (as opposed to some of the previous studies). It thus appears that top–down knowledge about the difficulty of an upcoming event is insufficient to drive changes in parietal alpha power (but also see Herrmann et al. (2023), indicating additional complexities). Palva and Palva (2011) suggest that distinguishing between endogenous and exogenous task demands is critical to understanding alpha-power dynamics. Manipulation of task demand via the saliency of a stimulus is an exogenous manipulation (Obleser et al., 2012; Petersen et al., 2015; Wöstmann et al., 2015; Wisniewski et al., 2017), whereas adjusting expectations about the demand level is an endogenous manipulation (present study). Therefore, we suggest that changes in alpha power due to

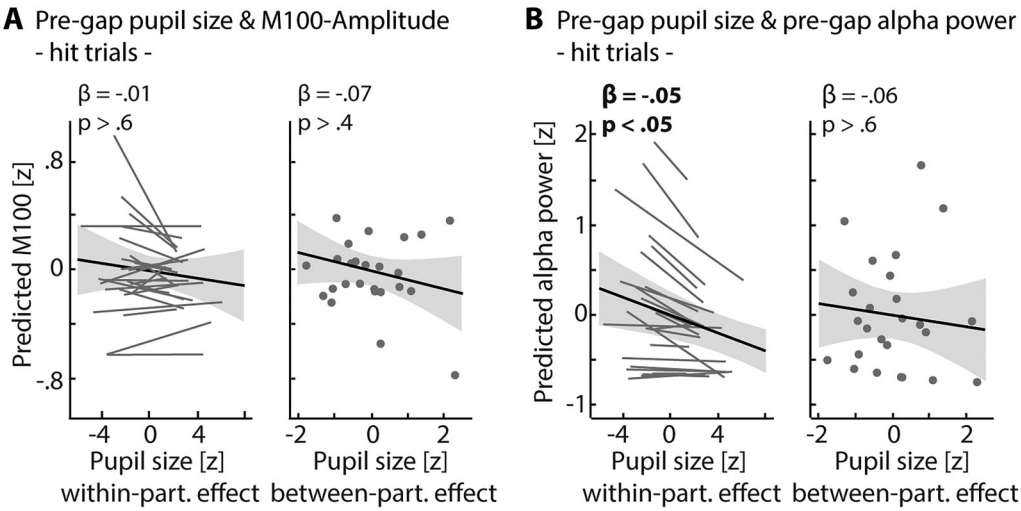

Figure 8. Relation between the pupil size and brain measures. ***A***, Relation between the pregap pupil size and M100 amplitude. LMM controlled for experimental conditions and was done on hit trials only. The pupil size was averaged across 0.5 s before the gap onset and baseline-corrected to the baseline window before the trial. M100 data were averaged across temporal sensors. No within-participant nor between-participant effect of the pupil size on the M100 amplitude was found. ***B***, Relation between the pregap pupil size and pregap parietal alpha power. LMM controlled for experimental conditions and was done on hit trials only. The pupil size was averaged across 0.5 s before the gap onset and baseline-corrected to the baseline window before the trial. Alpha-power data were averaged across the same 0.5 s time window and across parietal sensors. A significant negative relationship between the pupil size and alpha power was found on a within-participant level.

listening demand may only be observed under specific task and stimulus conditions but do not generally vary with different levels of cognitive resource recruitment during listening.

Not auditory sensory processing but poststimulus alpha power is modulated by motivational state

Auditory sensory responses (M100 amplitude) were enhanced for a long compared with a short gap duration—and thus for the more salient target—but not for variations in motivation. The M100 and the N100, the electric equivalent, are known to respond most strongly to changes in physical stimulus properties (Hansen and Hillyard, 1980; Näätänen and Picton, 1987; Paiva et al., 2016; Frank et al., 2020). Nevertheless, attentional modulations of the M100/N100 have been observed previously but often limited to spatial tasks (Hillyard et al., 1973; Woldorff and Hillyard, 1991; Ding and Simon, 2012; O'Sullivan et al., 2015; Kraus et al., 2021; Orf et al., 2023). It appears, however, that the attentional boost through motivation is insufficient to affect auditory sensory responses.

In contrast to the auditory sensory processing, we observed a response-related neural signal that scaled with task difficulty and reward prospect. Research on the impact of reward on stimulus processing often focuses on the feedback-related negativity (FRN). The FRN is a component that peaks ~200 ms after the feedback about an earned or lost reward (Holroyd and Coles, 2002; Glazer et al., 2018). The FRN is thought to scale with the degree to which the actual feedback deviates from the expected feedback (Sambrook and Goslin, 2015; Frömer et al., 2021) and is modulated by reward expectation (M. X. Cohen et al., 2007). In the present study, participants knew whether they were in a reward-irrelevant or a reward-relevant trial and how difficult target detection was. Moreover, the response participants made upon gap detection was the only feedback that they received about possibly gaining a reward. Detecting a gap in hard trials may have led to a more unexpected feedback signal (i.e., positive surprise) than in easy trials because participants knew that it would be less likely for them to detect the gap in hard trials. This feedback signal may be greater in the reward-relevant than the reward-irrelevant condition. We, therefore, interpret the observed effect of motivation as a positive surprise related to the detection of the gap.

Although there was no change in pregap alpha power nor in auditory sensory processing (M100) due to changes in the motivational state, the postgap alpha-power suppression was stronger during high compared with low motivation, independently of task demand. The suppression of alpha power is thought to be a sign of the facilitation, and therefore gating, of the processing of sensory input (Pfurtscheller, 2003; Klimesch et al., 2007; Jensen and Mazaheri, 2010; Palva and Palva, 2011). In visual attention tasks, reward prospect enhanced post-target encoding (Hall-McMaster et al., 2019) and neural processing in attention networks (Small et al., 2005), suggesting motivation influences of attentional top–down mechanisms on sensory processing. Both the response-related neural signal and the poststimulus alpha-power suppression suggest motivation affects top–down mechanisms during effortful listening.

Discrepancy between changes in the pupil size and alpha power

Both parietal alpha power and pupil size increased over the trial time course toward the gap, which proved beneficial for behavior. However, the degree to which both measures were affected by our experimental manipulations differed. The pupil size was greater for higher task demands and modulated by motivation, whereas parietal alpha power prior to the gap did not change for either manipulation.

Research investigating the relations between both metrics is rare. The few studies that observed simultaneous demand-driven dynamics in the pupil size and alpha power manipulated the demand via the stimulus itself, for example, by adding different levels of background noise to speech or using noise-vocoded speech at different levels (McMahon et al., 2016; Miles et al., 2017; Ala et al., 2020). As outlined above, the present study had no acoustic differences in the pregap analysis window, which

may explain the absence of alpha-power changes. In a recent study using the same auditory paradigm in an audiovisual dual-task, we also found that changes driven by listening demands were more prominent in the pupil size than in parietal alpha power (Kraus et al., 2023b).

The current study also showed that the pregap pupil size and pregap parietal alpha power are negatively related (Kraus et al., 2023b). Although the pupil size and alpha power were differently sensitive to listening demand and motivation, a common underlying mechanism seems to affect both the pupil size and parietal alpha power but in opposite directions. NE dynamics originating from the LC may be one candidate. Pupil size variations are correlated with activity in the LC (Aston-Jones and Cohen, 2005b), and the pupil dilates in response to LC stimulation (Liu et al., 2017). Increased NE activity emerging from LC is linked to optimizing task performance and task engagement (Aston-Jones and Cohen, 2005a). The NE influence on thalamic modulations (McCormick, 1998) and the thalamic connection to cortical oscillatory activity (Steriade, 2000) provide evidence for a neural mechanism affecting both the pupil size and neural oscillatory alpha power (Dahl et al., 2022).

Conclusion

The present study confirms that the pupil size robustly indexes cognitive investment during listening and provides an integrated readout of an individual's motivational state. However, the neural mechanisms that encode listening demand and motivational state reveal a more nuanced picture: expectation of a more demanding or more important (i.e., reward-relevant) sensory input does not suffice to elicit variations in neural alpha power. Auditory sensory processing was also not affected by a listener's motivational state. Importantly, we observed that the known alpha-power suppression in the wake of an auditory target event appears amplified under top–down motivational regulation. In sum, while the pupil size poses an integrated readout of listening demand and motivation, both dimensions selectively affect sensory and attentional postprocessing aspects of auditory neurophysiology.

References

Ala TS, Graversen C, Wendt D, Alickovic E, Whitme WM, Lunner T (2020) An exploratory study of EEG alpha oscillation and pupil dilation in hearing-aid users during effortful listening to continuous speech. PLoS One 15:1–15.

Alavash M, Obleser J (2024) Brain network interconnectivity dynamics explain metacognitive differences in listening behavior. J Neurosci 44:31.

Alavash M, Tune S, Obleser J (2021) Dynamic large-scale connectivity of intrinsic cortical oscillations supports adaptive listening in challenging conditions. PLoS Biol 19:10.

Alday PM (2019) How much baseline correction do we need in ERP research? Extended GLM model can replace baseline correction while lifting its limits. Psychophysiology 56:1–14.

Alfandari D, Richter M, Wendt D, Fiedler L, Naylor G (2023) Previous mental load and incentives influence anticipatory arousal as indexed by the baseline pupil diameter in a speech-in-noise task. Trends Hear 27: 23312165231196520.

Aston-Jones G, Cohen JD (2005a) Adaptive gain and the role of the locus coeruleus-norepinephrine system in optimal performance. J Comp Neurol 493:99–110.

Aston-Jones G, Cohen JD (2005b) An integrative theory of locus coeruleus-norepinephrine function: adaptive gain and optimal performance. Annu Rev Neurosci 28:403–450.

Baines S, Ruz M, Rao A, Denison R, Nobre AC (2011) Modulation of neural activity by motivational and spatial biases. Neuropsychologia 49:2489–2497.

Banerjee S, Snyder AC, Molholm S, Foxe JJ (2011) Oscillatory alpha-band mechanisms and the deployment of spatial attention to anticipated auditory and visual targetlocations: supramodal or sensory-specific control mechanisms? J Neurosci 31:9923–9932.

Behrmann M, Geng JJ, Shomstein S (2004) Parietal cortex and attention. Curr Opin Neurobiol 14:212–217.

Bell A, Fairbrother M, Jones K (2019) Fixed and random effects models: making an informed choice. Qual Quant 53:1051–1074.

Benjamini Y, Hochberg Y (1995) Controlling the false discovery rate: a practical and powerful approach to multiple testing. J R Stat Soc Series B Stat Methodol 57:289–300.

Bijleveld E, Custers R, Aarts H (2009) The unconscious eye opener. Psychol Sci 20:1313–1315.

Brehm JW, Self EA (1989) The intensity of motivation. Annu Rev Psychol 40: 109–131.

Cohen J (1988) *Statistical power analysis for the behavioral sciences*, Ed. 2, pp 20–26. Hillsdale, NJ: Lawrence Erlbaum Associates.

Cohen MX (2014) *Analyzing neural time series data: theory and practice*. Cambridge, MA: MIT press.

Cohen MX, Elger CE, Ranganath C (2007) Reward expectation modulates feedback-related negativity and EEG spectra. Neuroimage 35:968–978.

Cole L, Lightman S, Clark R, Gilchrist ID (2022) Tonic and phasic effects of reward on the pupil: implications for locus coeruleus function. Proc Biol Sci 289:20221545.

Crosse MJ, Di Liberto GM, Bednar A, Lalor EC (2016) The multivariate temporal response function (mTRF) toolbox: a MATLAB toolbox for relating neural signals to continuous stimuli. Front Hum Neurosci 10:1–14.

Dahl MJ, Mather M, Werkle-Bergner M (2022) Noradrenergic modulation of rhythmic neural activity shapes selective attention. Trends Cogn Sci 26: 38–52.

Dienes Z (2014) Using Bayes to get the most out of non-significant results. Front Psychol 5:1–17.

Dimitrijevic A, Smith ML, Kadis DS, Moore DR (2017) Cortical alpha oscillations predict speech intelligibility. Front Hum Neurosci 11:88.

Ding N, Simon JZ (2012) Neural coding of continuous speech in auditory cortex during monaural and dichotic listening. J Neurophysiol 107:78–89.

Frank M, Muhlack B, Zebe F, Scharinger M (2020) Contributions of pitch and spectral information to cortical vowel categorization. J Phon 79:100963.

Frömer R, Nassar MR, Bruckner R, Stürmer B, Sommer W, Yeung N (2021) Response-based outcome predictions and confidence regulate feedback processing and learning. Elife 10:1–29.

Glasser MF, et al. (2017) Manuscripts a multi-modal parcellation of human cerebral cortex. Nature 536:171–178.

Glazer JE, Kelley NJ, Pornpattananangkul N, Mittal VA, Nusslock R (2018) Beyond the FRN: broadening the time-course of EEG and ERP components implicated in reward processing. Int J Psychophysiol 132:184–202.

Goldstein RZ, Cottone LA, Jia Z, Maloney T, Volkow ND, Squires NK (2006) The effect of graded monetary reward on cognitive event-related potentials and behavior in young healthy adults. Int J Psychophysiol 62: 272–279.

Gross J, Kujala J, Hämäläinen M, Timmermann L, Schnitzler A, Salmelin R (2001) Dynamic imaging of coherent sources: studying neural interactions in the human brain. Proc Natl Acad Sci USA 98:694–699.

Hall-McMaster S, Muhle-Karbe PS, Myers NE, Stokes MG (2019) Reward boosts neural coding of task rules to optimize cognitive flexibility. J Neurosci 39:8549–8561.

Hämäläinen M (1995) Functional localization based on measurements with a whole-head magnetometer system. Brain Topogr 7:283–289.

Hansen JC, Hillyard SA (1980) Endogeneous brain potentials associated with selective auditory attention. Electroencephalogr Clin Neurophysiol 49: 277–290.

Henry MJ, Herrmann B, Kunke D, Obleser J (2017) Aging affects the balance of neural entrainment and top-down neural modulation in the listening brain. Nat Commun 8:15801.

Henry MJ, Herrmann B, Obleser J (2014) Entrained neural oscillations in multiple frequency bands comodulate behavior. Proc Natl Acad Sci USA 111:14935–14940.

Henry MJ, Obleser J (2012) Frequency modulation entrains slow neural oscillations and optimizes human listening behavior. Proc Natl Acad Sci USA 109:20095–20100.

Herrmann B, Johnsrude IS (2020) A model of listening engagement (MoLE). Hear Res 397:108016.

Herrmann B, Maess B, Henry MJ, Obleser J, Johnsrude IS (2023) Neural signatures of task-related fluctuations in auditory attention and age-related changes. Neuroimage 268:119883.
Herrmann B, Ryan JD (2024) Pupil size and eye movements differently index effort in both younger and older adults. J Cogn Neurosci 36:1325–1340.
Hillyard SA, Hink RF, Schwent VL, Picton TW (1973) Electrical signs of selective attention in the human brain. Science 182:177–180.
Holroyd CB, Coles MGH (2002) The neural basis of human error processing: reinforcement learning, dopamine, and the error-related negativity. Psychol Rev 109:679–709.
Jensen O, Mazaheri A (2010) Shaping functional architecture by oscillatory alpha activity: gating by inhibition. Front Hum Neurosci 4:1–8.
Joshi S, Gold JI (2020) Pupil size as a window on neural substrates of cognition. Trends Cogn Sci 24:466–480.
Joshi S, Li Y, Kalwani RM, Gold JI (2016) Relationships between pupil diameter and neuronal activity in the locus coeruleus, colliculi, and cingulate cortex. Neuron 89:221–234.
Kadem M, Herrmann B, Rodd JM, Johnsrude IS (2020) Pupil dilation is sensitive to semantic ambiguity and acoustic degradation. Trends Hear 24: 2331216520964068.
Kahneman D, Beatty J (1966) Pupil diameter and load on memory. Science 154:1583–1586.
Keitel A, Gross J (2016) Individual human brain areas can be identified from their characteristic spectral activation fingerprints. PLoS Biol 14:1–22.
Klimesch W, Sauseng P, Hanslmayr S (2007) EEG alpha oscillations: the inhibition-timing hypothesis. Brain Res Rev 53:63–88.
Koelewijn T, Zekveld AA, Festen JM, Kramer SE (2012) Pupil dilation uncovers extra listening effort in the presence of a single-talker masker. Ear Hear 33:291–300.
Koelewijn T, Zekveld AA, Lunner T, Kramer SE (2018) The effect of reward on listening effort as reflected by the pupil dilation response. Hear Res 367:106–112.
Kraus F, Obleser J, Herrmann B (2023a) Pupil size sensitivity to listening demand depends on motivational state. eNeuro 10:1–12.
Kraus F, Tune S, Obleser J, Herrmann B (2023b) Neural α oscillations and pupil size differentially index cognitive demand under competing audiovisual task conditions. J Neurosci 43:4352–4364.
Kraus F, Tune S, Ruhe A, Obleser J, Wöstmann M (2021) Unilateral acoustic degradation delays attentional separation of competing speech. Trends Hear 25:23312165211013242.
Krebs RM, Boehler CN, Appelbaum LG, Woldorff MG (2013) Reward associations reduce behavioral interference by changing the temporal dynamics of conflict processing. PLoS One 8:e53894.
Liu Y, Rodenkirch C, Moskowitz N, Schriver B, Wang Q (2017) Dynamic lateralization of pupil dilation evoked by locus coeruleus activation results from sympathetic, not parasympathetic, contributions. Cell Rep 20: 3099–3112.
Mathôt S, Fabius J, Van Heusden E, Van der Stigchel S (2018) Safe and sensible preprocessing and baseline correction of pupil-size data. Behav Res Methods 50:94–106.
Mazaheri A, van Schouwenburg MR, Dimitrijevic A, Denys D, Cools R, Jensen O (2014) Region-specific modulations in oscillatory alpha activity serve to facilitate processing in the visual and auditory modalities. Neuroimage 87:356–362.
McCormick DA (1998) Cholinergic and noradrenergic modulation of thalamocortical processing. Trends Neurosci 12:215–221.
McMahon CM, Boisvert I, de Lissa P, Granger L, Ibrahim R, Lo CY, Miles K, Graham PL (2016) Monitoring alpha oscillations and pupil dilation across a performance-intensity function. Front Psychol 7:1–12.
Miles K, McMahon C, Boisvert I, Ibrahim R, de Lissa P, Graham P, Lyxell B (2017) Objective assessment of listening effort: coregistration of pupillometry and EEG. Trends Hear 21:1–13.
Näätänen R, Picton T (1987) The N1 wave of the human electric and magnetic response to sound: a review and an analysis of the component struture. Psychophysiology 24:375–425.
Niemi P, Näätänen R (1981) Foreperiod and simple reaction time. Psychol Bull 89:133–162.
Nobre A, Correa A, Coull J (2007) The hazards of time. Curr Opin Neurobiol 17:465–470.
Obleser J, Wöstmann M, Hellbernd N, Wilsch A, Maess B (2012) Adverse listening conditions and memory load drive a common alpha oscillatory network. J Neurosci 32:12376–12383.
Ohlenforst B, Wendt D, Kramer SE, Naylor G, Zekveld AA, Lunner T (2018) Impact of SNR, masker type and noise reduction processing on sentence recognition performance and listening effort as indicated by the pupil dilation response. Hear Res 365:90–99.
Ohlenforst B, Zekveld AA, Lunner T, Wendt D, Naylor G, Wang Y, Versfeld NJ, Kramer SE (2017) Impact of stimulus-related factors and hearing impairment on listening effort as indicated by pupil dilation. Hear Res 351:68–79.
Oostenveld R, Fries P, Maris E, Schoffelen JM (2011) Fieldtrip: open source software for advanced analysis of MEG, EEG, and invasive electrophysiological data. Comput Intell Neurosci 2011:156869.
Orf M, Wöstmann M, Hannemann R, Obleser J (2023) Target enhancement but not distractor suppression in auditory neural tracking during continuous speech. IScience 26:106849.
O'Sullivan JA, Power AJ, Mesgarani N, Rajaram S, Foxe JJ, Shinn-Cunningham BG, Slaney M, Shamma SA, Lalor EC (2015) Attentional selection in a cocktail party environment can be decoded from single-trial EEG. Cereb Cortex 25:1697–1706.
Paiva TO, Almeida PR, Ferreira-Santos F, Vieira JB, Silveira C, Chaves PL, Barbosa F, Marques-Teixeira J (2016) Similar sound intensity dependence of the N1 and P2 components of the auditory ERP: averaged and single trial evidence. Clin Neurophysiol 127:499–508.
Palva S, Palva JM (2011) Functional roles of alpha-band phase synchronization in local and large-scale cortical networks. Front Psychol 2:204.
Parro C, Dixon ML, Christoff K (2018) The neural basis of motivational influences on cognitive control. Hum Brain Mapp 39:5097–5111.
Paul BT, Chen J, Le T, Lin V, Dimitrijevic A (2021) Cortical alpha oscillations in cochlear implant users reflect subjective listening effort during speech-in-noise perception. PLoS One 16:1–22.
Petersen EB, Wöstmann M, Obleser J, Stenfelt S, Lunner T (2015) Hearing loss impacts neural alpha oscillations under adverse listening conditions. Front Psychol 6:1–11.
Pfurtscheller G (2003) Induced oscillations in the alpha band: functional meaning. Epilepsia 44:2–8.
Pichora-Fuller MK, et al. (2016) Hearing impairment and cognitive energy: the framework for understanding effortful listening (FUEL). Ear Hear 37:5S–27S.
Richter M (2016) The moderating effect of success importance on the relationship between listening demand and listening effort. Ear Hear 37: 111S–117S.
Richter M, Gendolla GHE, Wright RA (2016) Three decades of research on motivational intensity theory. In: *Advances in motivation science* (Elliot AJ, ed), pp 149–186. Amsterdam: Elsevier.
Rushworth MFS, Paus T, Sipila PK (2001) Attention systems and the organization of the human parietal cortex. J Neurosci 21:5262–5271.
Sambrook TD, Goslin J (2015) A neural reward prediction error revealed by a meta-analysis of ERPs using great grand averages. Psychol Bull 141:213–235.
Sawaki R, Luck SJ, Raymond JE (2015) How attention changes in response to incentives. J Cogn Neurosci 27:2229–2239.
Small DM, Gitelman D, Simmons K, Bloise SM, Parrish T, Mesulam MM (2005) Monetary incentives enhance processing in brain regions mediating top-down control of attention. Cereb Cortex 15:1855–1865.
Steriade M (2000) Corticothalamic resonance, states of vigilance and mentation. Neuroscience 101:243–276.
Teoh YY, Yao Z, Cunningham WA, Hutcherson CA (2020) Attentional priorities drive effects of time pressure on altruistic choice. Nat Commun 11:3534.
Tune S, Alavash M, Fiedler L, Obleser J (2021) Neural attentional-filter mechanisms of listening success in middle-aged and older individuals. Nat Commun 12:1–14.
Tusche A, Hutcherson CA (2018) Cognitive regulation alters social and dietary choice by changing attribute representations in domain-general and domain-specific brain circuits. Elife 7:1–35.
van den Berg B, Krebs RM, Lorist MM, Woldorff MG (2014) Utilization of reward-prospect enhances preparatory attention and reduces stimulus conflict. Cogn Affect Behav Neurosci 14:561–577.
Vazey EM, Moorman DE, Aston-Jones G (2018) Phasic locus coeruleus activity regulates cortical encoding of salience information. Proc Natl Acad Sci USA 115:E9439–E9448.
Vrba J, Robinson SE (2001) Signal processing in magnetoencephalography. Methods 25:249–271.
Wagenmakers EJ (2007) A practical solution to the pervasive problems of p values. Psychon Bull Rev 14:779–804.

Weisz N, Hartmann T, Müller N, Lorenz I, Obleser J (2011) Alpha rhythms in audition: cognitive and clinical perspectives. Front Psychol 2:1–15.

Wendt D, Dau T, Hjortkjær J (2016) Impact of background noise and sentence complexity on processing demands during sentence comprehension. Front Psychol 7:1–12.

Winn MB, Edwards JR, Litovsky RY (2015) The impact of auditory spectral resolution on listening effort revealed by pupil dilation. Ear Hear 36:1–31.

Wisniewski MG, Thompson ER, Iyer N (2017) Theta- and alpha-power enhancements in the electroencephalogram as an auditory delayed match-to-sample task becomes impossibly difficult. Psychophysiology 54:1916–1928.

Woldorff MG, Hillyard SA (1991) Modulation of early auditory processing during selective listening to rapidly presented tones. Electroencephalogr Clin Neurophysiol 79:170–191.

Wöstmann M, Herrmann B, Wilsch A, Obleser J (2015) Neural alpha dynamics in younger and older listeners reflect acoustic challenges and predictive benefits. J Neurosci 35:1458–1467.

Wöstmann M, Lim SJ, Obleser J (2017) The human neural alpha response to speech is a proxy of attentional control. Cereb Cortex 27:3307–3317.

Yee DM, Braver TS (2018) Interactions of motivation and cognitive control. Curr Opin Behav Sci 19:83–90.

Zekveld AA, Kramer SE (2014) Cognitive processing load across a wide range of listening conditions: insights from pupillometry. Psychophysiology 51: 277–284.

Zekveld AA, Kramer SE, Festen JM (2010) Pupil response as an indication of effortful listening: the influence of sentence intelligibility. Ear Hear 31: 480–490.

Zhang M, Siegle GJ, McNeil MR, Pratt SR, Palmer C (2019) The role of reward and task demand in value-based strategic allocation of auditory comprehension effort. Hear Res 381:107775.